U.S. DEPARTMENT OF THE INTERIOR

U.S. GEOLOGICAL SURVEY

Rebound in the Pierre Shale of South Dakota and Colorado —

Field and laboratory evidence of physical conditions related

to processes of shale rebound

by   )

THOMAS C. NICHOLS, JR.[1]

Open-File Report 92-440

[1]Golden, Colorado

1992

Contents

Page

Illustrations

Contents (Continued)

Illustrations (Continued)

Tables

Abstract

In areas of outcropping Pierre Shale (an overconsolidated smectitic shale) in central South Dakota, and in suburbs southwest of greater Denver, Colorado, numerous dwelling and highway foundations have suffered mild to major damage caused by heaving soils and bedrock. An assessment is made of the possible contribution of bedrock rebound to excessive structural damage often difficult to explain by swelling soils. Profiles of measured geotechnical and geophysical properties were determined for sections of the shale as much as 180 m deep that suggest rebound in the shale consists primarily of volume expansion (increase of void volume) caused by expanding clay fabric. The profiles reflect rebound that has taken place as a result of natural erosional unloading and also rebound that may take place as a result of future unloading caused by engineering excavations. Compared to the unweathered, saturated shale at depth, the overlying weathered shale becomes progressively less dense, more porous, and less saturated, but generally contains more pore water toward the upper boundary of the bedrock surface. The profiles suggest that the shale is expanding upward with time.

Even though the shale is an overconsolidated smectitic clay shale, hydration of the clays may not be the major cause of rebound volume increase. The profiles show that the increase of void volume nearly always appears to precede the inflow of new pore water and exceed its volume. The clay minerals determined for the Colorado profile were dominantly smectites with divalent exchange ions such as Ca^{2+}, which would tend to limit their swelling potential. Because the clays on the profile become less saturated as they expand and because of their limited swelling potential, volume changes due to hydration of the clays are likely to be less than those caused by recoverable strain energy released as clay bonds are relaxed by weathering and deformation.

Introduction

The rebound of overconsolidated clay shale bedrock caused by engineering excavations can cause serious foundation problems to dwellings and roadways. Damage done by heaving bedrock (rebound) generally has not been distinguished from damage caused by swelling soils derived from weathered bedrock, probably because most of the severe damage to engineered structures is thought to result from expanding clay soils upon absorption of water. At our field locations, quantitative field data describing the rebound behavior of shale bedrock are not as abundant as those that describe the behavior of the overlying swelling clay soils. Our studies suggest bedrock rebound does not necessarily require absorption of moisture, but rather depends on the removal of confining loads and the subsequent disturbance of the clay matrix, whereas, swelling of soil primarily requires the absorption of water. Rebound displacements commonly are not anticipated in engineering practice and,

therefore, are not considered in design. Consequently, a better understanding of rebound processes is needed so that engineering practice to mitigate rebound deformations can be substantially improved.

Because there may be more than one understanding of rebound among practitioners dealing with the problem of heaving and swelling soils, the definition of rebound (Nichols, 1980) used herein is "the expansive recovery of surficial crustal material, either instantaneous, or over time, or both, and is initiated by the removal or relaxation of superincumbent loads..." Rebound displacements allow elastic and inelastic relaxation of the crustal masses to occur. The long-term outward and upward movements associated with rebound are displacements related to relaxation processes of geological materials that are poorly understood, and the basis for predicting these displacements has not been clearly established. Not only are changes of stress important to the rebound process, but so are fabric, physical properties and anisotropy of the geologic materials, strain energy stored in the fabric by past and present geologic loads, and external environmental influences such as water and temperature (Nichols, 1980; Nichols and Collins, 1991). The problem of rebound is one with which engineers must deal whenever the equilibrium of geological materials is disturbed, especially in large excavations. In areas where rebound deformations can significantly affect engineering structures, it is desirable to understand rebound behavior and to determine practical guidelines for prediction of the short- and long-term consequences of rebound.

Rebound in this text is considered to be the expansive recovery of the overconsolidated Pierre Shale in response to natural or engineering excavations of overburden loads. Rebound displacements in the shale consist of expansive elastic and time-dependent anelastic components that commonly occur after excavation of overlying loads.

Data obtained during geotechnical and geophysical investigations of the Pierre Shale in South Dakota and Colorado (Nichols and Collins, 1986; Nichols and others, 1986; Collins and Nichols, 1987; Nichols and others, 1988; Collins and others, 1988; Nichols, 1991) have revealed some of the physical aspects of the rebound process in the overconsolidated shale. Some of these data are used here to assess the natural rebound process and the possible contribution of rebound deformations to the severe damage of dwelling foundations and local roadways in the areas of concern.

Previous work—Pierre Shale

During the construction of the Oahe Dam on the Missouri River 16 km northwest of Pierre, South Dakota (fig. 1), the U.S. Army Corps of Engineers observed time-dependent vertical ground offsets up to 0.3 m in the flat-lying Pierre Shale (smectitic clay shale) that crops out extensively in the region.
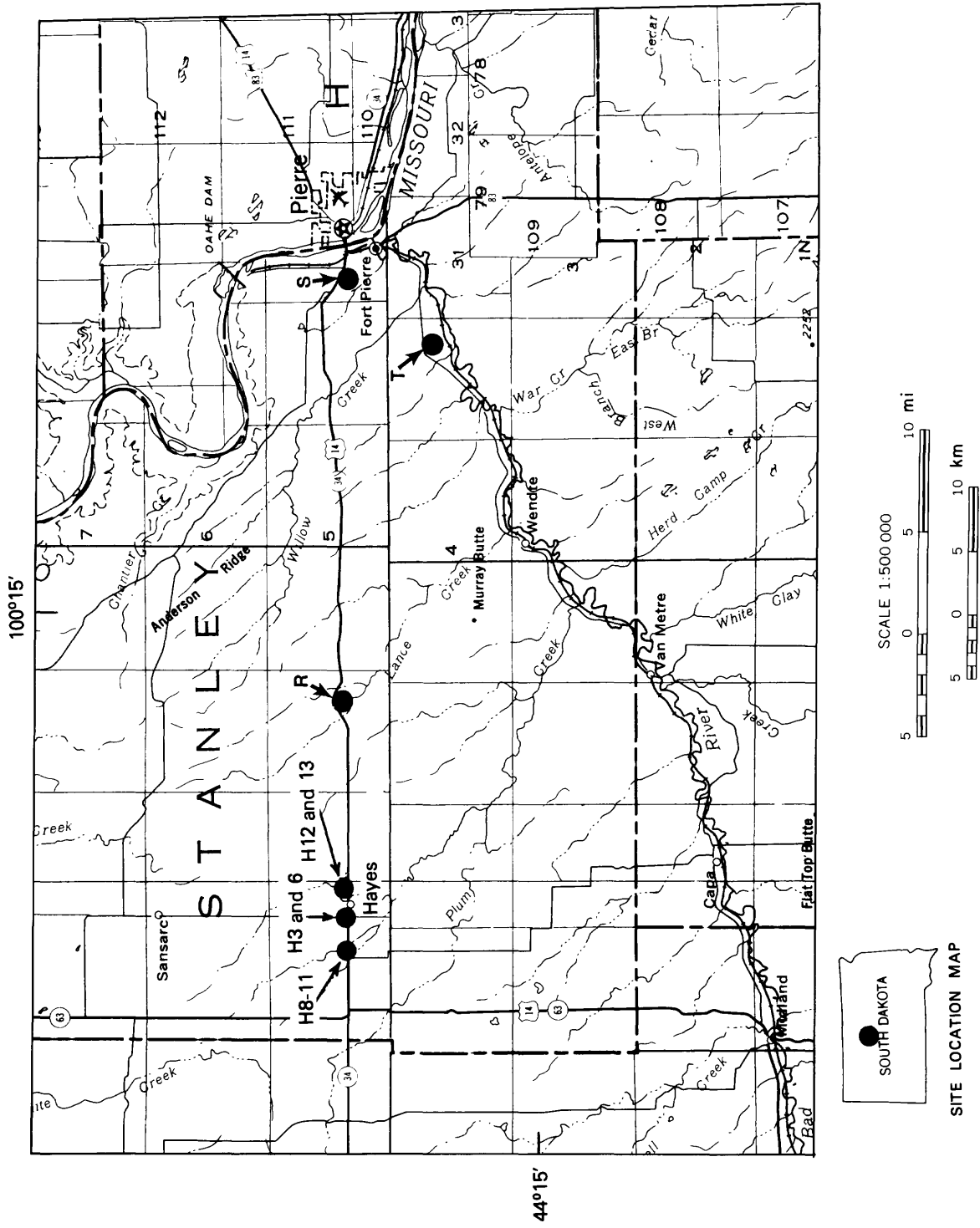
2

Figure 1—Map showing drill sites H8, H10, H11, H12, and H13; trench sites R, S, and T: and the location of the Oahe Dam near Pierre, South Dakota.

Approximately a month after massive excavations for the dam stilling basin were finished (Underwood and others, 1964), abrupt rebound displacements along pre-existing, steeply dipping fault planes on the floor of the basin were detected over a period of 3 days. These were followed by time-dependent displacements that were measured for a year. The U.S. Army Corps of Engineers successfully modified the design of the dam to compensate for any future rebound deformations. The foundation investigations carried out by Underwood and others (1964) and nearby geotechnical investigations conducted in the Pierre Shale by the U.S. Geological Survey (Nichols and others, 1986; Collins and others, 1988) indicate that continuing differential rebound displacements are significantly influenced by pre-existing fault planes. Engineering practice used to mitigate time-dependent rebound damage to highways recently constructed over pre-existing faults in the Pierre Shale of South Dakota has not been completely successful.

Outcropping Pierre Shale along the western and southwestern perimeter of the Denver, Colorado, metropolitan area is the source of severe foundation problems and road damage in recently developed communities and highways. Much of the damage is caused by swelling clay soils and heaving bedrock (rebound) associated with weathering and erosion of the Pierre Shale (generally a smectitic clay shale in this area). Preliminary investigations by Nichols (1991) suggest that rebound may contribute significantly to some of the observed damage.

In the area of concern (fig. 2), beds of the Pierre Shale (approximately 2.10 km thick) dip steeply eastward (greater than 45°) as a result of regional uplift and, except where locally covered by alluvial deposits, crop out for a width of at least 2.4 km in an east-west direction and for many kilometers along a north-south strike direction. Several new subdivisions built since the early 1970's in the area, bounded by Quincy Avenue on the north, Colorado State Highway C470 on the west, Simms Avenue on the east, and Belleview Avenue on the south, have had a history of continuing excessive damage to foundations, roadways, and utility lines. Kline (1982) conducted a multivariable analysis of independent construction variables in this area that may have contributed to the prediction of foundation damage, the dependent variable. The independent variables were house style, foundation type, depth to bedrock, soil type, and age. He concluded that only the age of the house and the depth to bedrock were significant in predicting house damage. Both of these construction variables, simultaneously influencing foundation damage, imply that time-dependent deformations caused by the disturbance of the shale during construction are a result of rebound, and, in this locality, the removal of overlying surficial or weathered shale deposits may have caused significant rebound deformations.

In addition, a major regional geologic structure, the Golden fault, extends into the area of severe damage (fig. 1 and plate V in Kline, 1982); tectonic fault displacements on this structure may have occurred as recently as Quaternary time (Kirkham and Rogers, 1981). Even though an examination
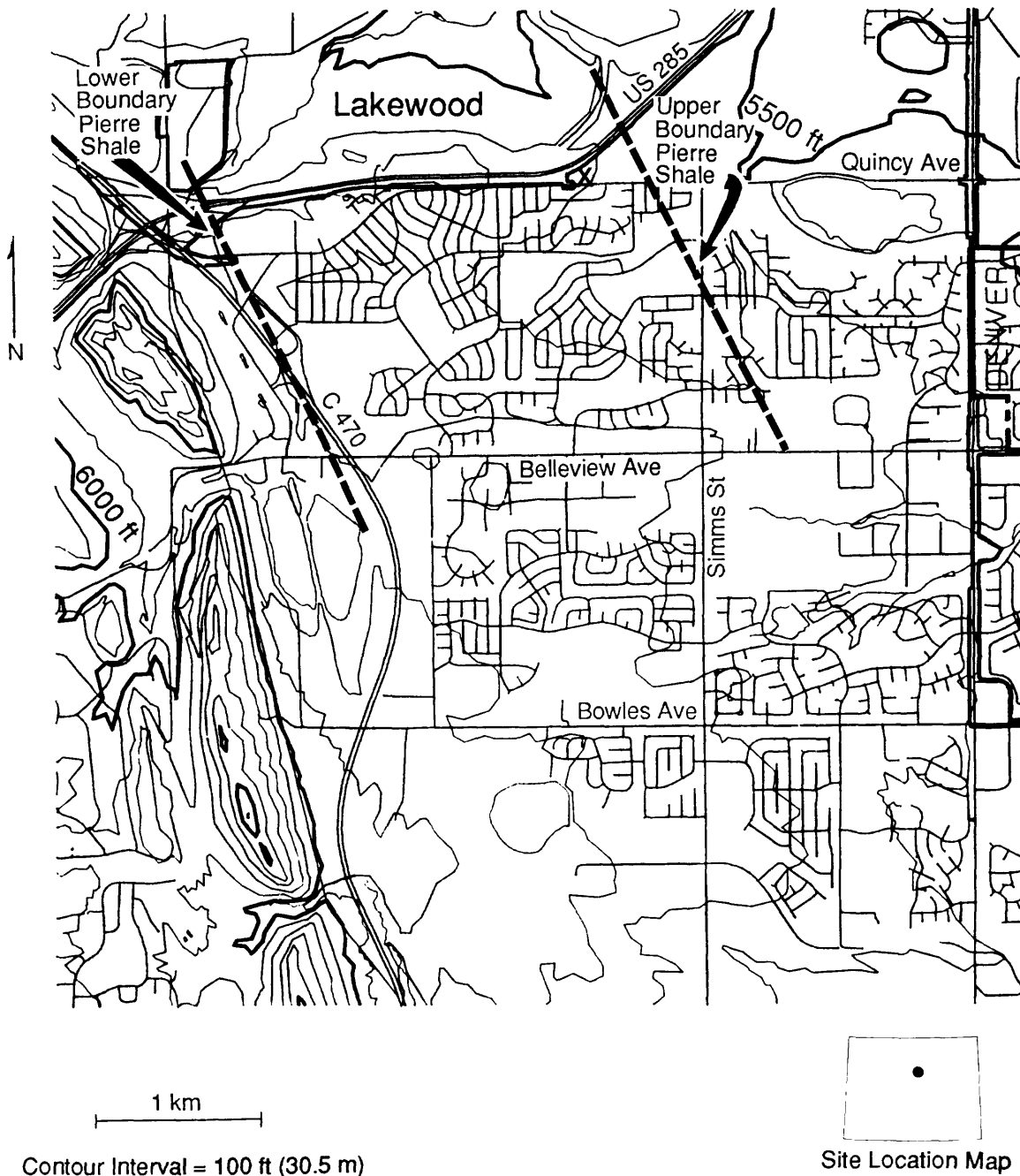
4

Figure 2–Map showing area of damaged homes, Quincy Avenue on north, Simms Street on east, Belleview Avenue on south, and Colorado State Highway C470 on west. Upper and lower boundaries of outcropping Pierre Shale in the area also are approximately located (after Scott, 1972). X marks location of site investigation (Fig. 4).

5

of aerial photographs taken in 1937, 1949, 1964, 1971, and 1972 shows no geomorphic evidence of recent movement along the fault trace, past disturbances causing non-uniform fracture densities across the fault may contribute significantly to differential rebound displacements along parallel linear trends upon excavation of the surrounding shale.

Field and laboratory data obtained during geotechnical and geophysical investigations of the Pierre Shale in South Dakota and Colorado (Nichols and others, 1986; Nichols and Collins, 1986; Collins and Nichols, 1987; Nichols and others, 1988; Collins and others, 1988; Nichols, 1991) have revealed some of the physical aspects of the rebound process in the overconsolidated shale. This report presents published and unpublished data and conclusions from the South Dakota and Colorado studies conducted to assess the rebound process and the contribution of rebound deformations to the severe damage of dwelling foundations and local roadways in the areas of concern.

Geotechnical investigations—South Dakota

Near-surface physical properties data (table 1) were determined on weathered samples from three shallow trenches (R, S, and T in fig. 1) west of Pierre, South Dakota. The trenches were excavated on highway slopes of outcropping shale modified for new highway construction or repairs by the removal as much as 8.5 m of weathered flat-lying shale. Other physical properties data (Nichols and others, 1986) determined on unweathered samples from depths to 180 m in core hole H12 near Hayes, South Dakota (fig. 1), are shown on table 2. The members of the Pierre Shale (Crandell, 1958) from which the samples were taken are also identified in these tables.

Bulk density, water content, grain density, degree of saturation, and grain-size determinations were made on samples from the trenches and the core hole. Bulk density and moisture content determinations were made with portable laboratory equipment set up at each field site, and other determinations were made in standard laboratory facilities. Of the samples tested from the core hole (Nichols and others, 1986), all but one were taken from the fresh, unweathered, typically unfractured bedrock, a dark-grey claystone below the weathered zone (visually defined by the presence of chemical weathering), whereas samples tested from the trenches were unfractured, intact pieces of weathered bedrock, all taken at shallow depths in the weathered zone. The weathered bedrock generally is slightly to highly fractured claystone, with fractures generally filled or coated by gypsum, calcite, iron, or manganese oxides. The fractured segments of bedrock have oxidation rinds, the thickness depending on the local degree of fracturing and oxidation. Zones of brecciated claystone covered with slickensides were common. The sample taken at 23 m in core hole H12 was from the base of the weathered zone.

6

TABLE 1. Weathered samples taken from trenches dug west of Pierre, South Dakota

[Data are averaged for each sample group. One sample at 23.2 m depth is taken from the lower weathered zone in the deep core hole, H-12]

Pierre Shale member sampled	No. of samples	Depth interval of samples (m)	Trench location (site, section, township, and range)	Bulk density (g/cm^3)	Porosity (percent)	Moisture content (percent)	Degree of saturation (percent)
Mobridge	1	23.2	H-12 Sec. 22 T. 5 N. R. 26 E.	2.06	38	17.9	96
Upper part, Virgin Creek	9	2.3-9.1	R Sec. 23 T. 5 N. R. 28 E.	1.88	48	22.9	91
Lower part, Virgin Creek	7	0.8-4.4	T Sec. 11 T. 4 N. R. 30 E.	1.89	46	22.7	93
Verendrye	4	5.8-9.8	S Sec. 20 T. 5 N. R. 31 E.	1.93	45	22.9	98
Verendrye	4	4.7-5.8	T Sec. 11 T. 4 N. R. 30 E.	2.00	41	19.5	96
DeGrey	3	6.3-9.3	S Sec. 20 T. 5 N. R. 31 E.	1.91	45	22.4	95
DeGrey	2	2.4-3.8	S Sec. 20 T. 5 N. R. 31 E.	1.86	48	24.2	93

TABLE 2. Unweathered samples cored from deep core hole (H-12) near Hayes, South Dakota

Pierre Shale member sampled	No. of samples	Depth interval of samples (m)	Bulk density (g/cc)	Porosity (percent)	Moisture content (percent)	Degree of saturation (percent)
Mobridge	3	32.3-47.9	2.16	34	15.0	99
Virgin Creek	5	55.5-84.1	2.12	37	17.3	101
Verendrye	4	93.3-116.2	2.16	33	15.7	102
DeGrey	8	123.8-181.1	2.14	36	17.1	101

The physical properties data in tables 1 and 2 show a comparison of bulk density, water content, porosity, and degree of saturation of the weathered samples from the trenches to the unweatheredsamples from the core hole. The data show that all of the weathered samples are less dense, are more porous fig. 3) and contain more water, but are less saturated than the unweathered samples. The core hole sample taken at the base of the weathered zone (table 1) has properties transitional between the deeper core hole samples and the shallow trench samples. There are no data from the weathered zone between a depth of 23 m and the shallow trenches.

The only apparent differences between the clay content of the unweathered samples taken from core hole H12 and the weathered samples taken from the three shallow trenches are the increased amount of mixed-layer illite found in the smectites and a slight increase of total clay in samples taken from the weathered zone (table 3), thus suggesting increased expandability of the weathered clays.

Geotechnical and Geophysical Investigations—Colorado

To evaluate possible destructive rebound deformations and their severity for the area shown in fig. 2, a single site of investigation was chosen adjacent to an area having a known high-density occurrence of structural damage (Kline, 1982). The site location (fig. 4) was chosen as close as feasible to the inferred location of the Golden fault (Scott, 1972) on terrain undisturbed by construction and yet with as little thickness of surficial deposits overlying the Pierre Shale as possible. A location intersecting the Golden fault would allow an evaluation of fabric deterioration caused by past geologic deformation. The near-surface geology was mapped and a profile of the clay mineralogy (table 4) and physical properties (table 5) of the Pierre Shale was determined for a trench (27 m long and 2.9-3.6 m deep) excavated perpendicular (N. 68° E.) to the strike (N. 22° W.) of the Pierre Shale, and for a core hole drilled on the trench to a depth of 27 m (fig. 4). Samples from the trench and the core hole were used to determine clay mineralogy, bulk density, grain density, water content, porosity, degree of saturation, Atterberg limits, and grain-size distribution (Nichols, 1991); the results are shown on tables 4 and 5. Some measurements were made with portable field-laboratory apparatus set up at the site location, and remaining measurements were made in standard laboratory facilities. Field measurements of moisture content and bulk density were made immediately after the extraction of samples in order to obtain values as near as possible to the undisturbed in-situ conditions. The data obtained give a complete profile of the weathered zone that extends to a depth of 24 m (fig. 5). Additional subsurface structural data were obtained from a 114-m-long, high-resolution seismic refraction profile (Williams and King, 1991) parallel to the excavated trench (fig. 4). The survey extended beyond the trench about 25 m to the west and 40 m to the east.
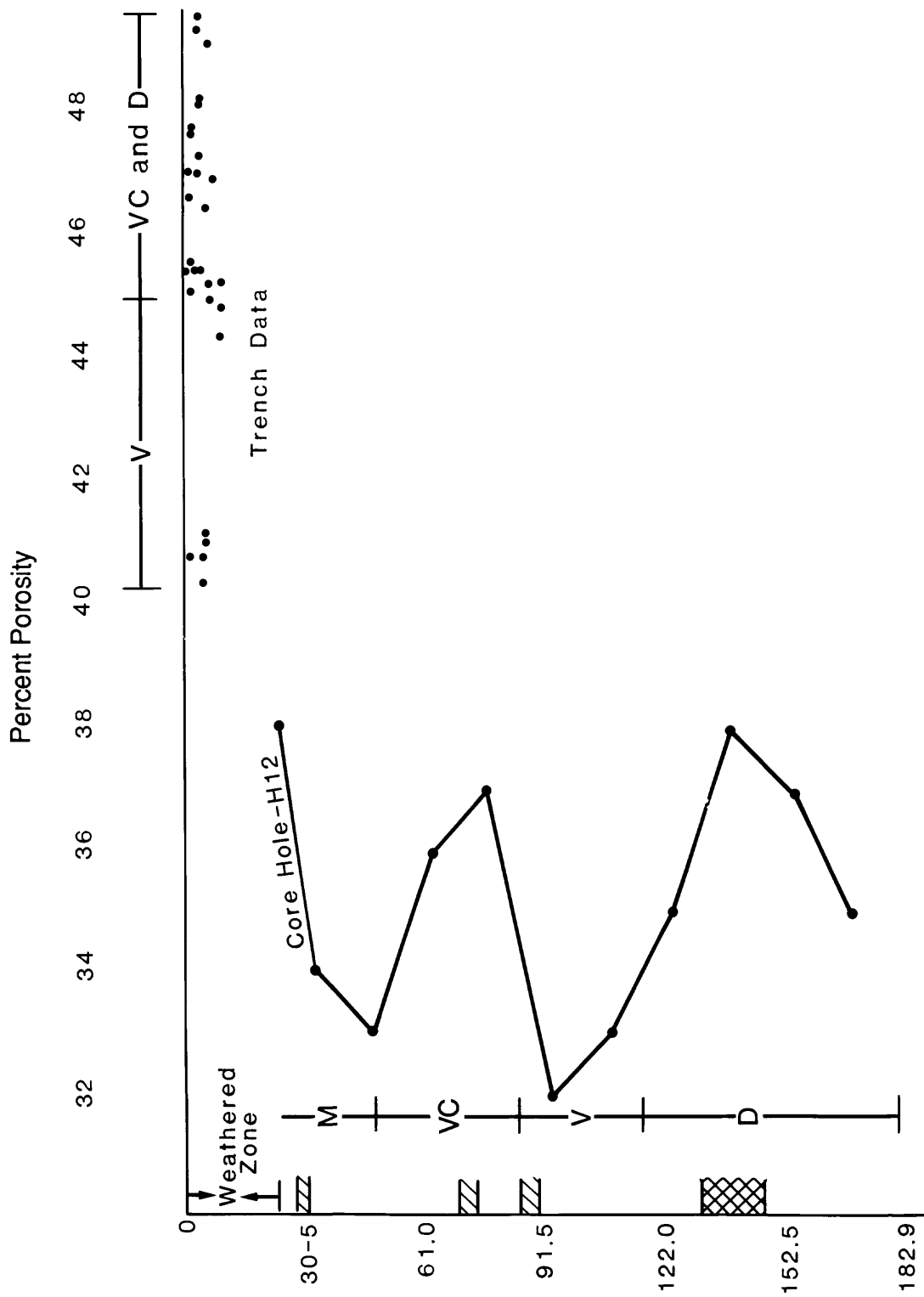
Figure 3—A comparison of depth to porosity determined from Pierre Shale samples taken from corehole H12 and trenches R, S, and T, located on Figure 1. ///// symbols show fracture zones, and XXXX symbol shows disturbed zone. M, VC, V and D represent the Mobridge, Virgin Creek, Verendrye, and DeGrey Members of the Pierre Shale.

TABLE 3. Clay mineralogy from X-ray analyses of Pierre Shale samples from central South Dakota[1]

Depth (m)	Member[2]	Site	Sample number	Percent I contained in I/s	Order of abundance Clay minerals	Total clay (percent)
0.85	V	Trench west of Pierre (S)	1	30	I/s, I, Ch, K	75
5.79	V	Do.	2	25	I/s, I, Ch, K	80
8.17	V	Do.	3	25	I/s, I, Ch, K	75
9.27	V	Do.	4	30	I/s, I, Ch, K	75
9.51	V	Do.	5	25	I/s, I, Ch=K	75
9.76	D	Do.	6	25	I/s, I, Ch	75
9.30	D	Do.	7	30	I/s, I	75
7.77	D	Do.	8	25	I/s, I, Ch	75
6.28	D	Do.	9	25	I/s, I, Ch=K	75
3.84	D	Do.	10	20	I/s, I, K, Ch	75
2.38	D	Do.	11	25	I/s, I, Ch	75
1.13	UVC	Trench Princes Ranch (R)	2	25	I/s, I, Ch, K	50
2.29	UVC	Do.	3	25	I/s, I, Ch, K	80
3.17	UVC	Do.	4	25	I/s, I, Ch	80

4.05	UVC	Do.	5	25	I/s, I, Ch	75
4.97	UVC	Do.	6	20	I/s, I, Ch, K	80
5.88	UVC	Do.	7	30	I/s, I, Ch	80
6.77	UVC	Do.	8	30	I/s, I, Ch, K	80
7.80	UVC	Do.	9	35	I/s, I, K, Ch	75
8.84	UVC	Do.	10	35	I/s, I, K. Ch	75
9.09	UVC	Do.	11	30	I/s, I, K, Ch	80
1.37	LVC	Trench on Bad River (T)	1	30	I/s, I	80
1.92	LVC	Do.	3	30	I/s, I, Ch=K	80
2.47	LVC	Do.	4	20	I/s, I, K, Ch	85
3.05	LVC	Do.	5	30	I/s, I, K, Ch	80
3.66	LVC	Do.	6	35	I/s, I, K, Ch	80
4.42	LVC	Do.	7	35	I/s, I, Ch, K	75
4.73	V	Do.	8	30	I/s, I, Ch, K	80
4.73	V	Do.	9	30	I/s, I, Ch=K	75
5.52	V	Do.	10	40	I/s, I, Ch=K	80
5.79	V	Do.	11	35	I/s, I, K, Ch	75
23.2	M	Core hole H-12	1	25	I/s, I, Ch, K	65
32.3	M	Do.	2	30	I/s, I, Ch, K	50
47.9	M	Do.	3	35	I/s, I, Ch, K	60
63.1	VC	Do.	4	15	I/s, I, Ch, K	70
78.4	VC	Do.	5	15	I/s, I, Ch	75
93.6	V	Do.	6	27	I/s, I, K, Ch	55

109.1	V	Do.	7	15	I/s, I, Ch=K	75
124.1	D	Do.	8	10	I/s, I, Ch, K	75
139.3	D	Do.	9	25	I/s, I, Ch, K	75
154.9	D	Do.	10	10	I/s, I, Ch	70
170.4	D	Do.	11	25	I/s, I, Ch, K	70

[1]X-ray analyses interpreted by L.G. Schultz, U.S. Geological Survey.

[2]Letters indicate members of Pierre Shale that were sampled.

M = Mobridge

UVC = Upper part, Virgin Creek

LVC = Lower part, Virgin Creek

V = Verendrye

D = DeGrey

[3]Symbols used: Ch = chlorite; I = illite; K = kaolinite; I/s = mixed

layer illite/smectite

Figure 4—Map Showing Approximate Extension of the Golden Fault
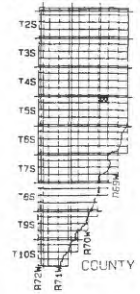and Site Location for Trench, Core Hole, and Seismic Reflection Line

TABLE 4.--Clay mineralogy from X-ray analyses of Pierre Shale samples from Colorado[1]

Sample[2]	Depth (m)	Clay fraction[3]	001 air-dried (Å)[4]	% expandable[4]	Coarse minerals[3]
1	2.5-4.0	I/S, I, K, C(?), Q(?)	13.13	80	Q, F, C, Go(?)
3A	--do--	I/S, I, K, C, Ch(?), F, Q	14.25	80	C, Q
3B	--do--	I/S, I, K, C, Ch(?), F, Q	14.16	80	Q, F
4	--do--	I/S, I, K, C, F, Q	13.56	80	C, Q
5	--do--	I/S, I, K, C, Ch(?), F, Q	14.26	80	C, Q
6A	--do--	I/S, I, K, C, F, Q	14.31	80	C, Q
7	--do--	I/S, I, K, C, Ch(?), F, Q	14.32	80	C, Q, F
8[5]	--do--	I/S, I, K, Ch, F, Q	14.24	90	Q, F
66	--do--	I/S, I, K, Ch, F, Q	14.25	80	Q, F
A4	--do--	I/S, I, K, C, Ch(?), F, Q	14.17	90	Q, F
C1	4.00	I/S, I, K, Ch(?), F, Q	14.36	80	Q, F, D(?)
C2	6.63	I/S, I, K, F, Q	14.19	80	Q, F, D(?)
C3-1	7.93	I/S, I, K, Ch(?), F, Q	14.15	80	N.A.
C5-1	10.21	I/S, I, K, F, Q	14.12	80	Q, F, D(?)
C6-2	13.11	I/S, I, K, F, Q	13.88	80	Q, F, D(?)
C7-2	16.07	I/S, I, K, F, Q	13.76	90	Q, F, D(?)
C8-4	18.60	I/S, I, K, F, Q	14.29	90	Q, F, D(?)
C9-2	22.56	I/S, I, K, F, Q	13.60	90	Q, F, D(?)
C9-5	23.48	I/S, I, K, F, Q	14.23	80	Q, F, D(?)
C10-3	25.30	I/S, I, K, Ch, F, Q	14.02	90	Q, F, D(?)
C10-6	25.91	I/S, I, K, Ch, F, Q	12.90	90	Q, F, D(?)

[1]X-ray analyses interpreted by D.D. Eberl, U.S. Geological Survey.

[2]Samples 1, 3A, 3B, 4, 5, 6A, 7, and 8 from the trench were taken from seams 1, 3, 4, 5, 6, 7, 8, and 10, respectively (fig. 5), and samples 66 and A4 were collected in the trench at the drill site. Samples C1 through C10-6 were core samples taken from the drill hole.

[3]Symbols used: C=calcite; Ch=chlorite; D=dolomite; F=feldspar; G=gypsum; Go=goethite; I=illite; I/S=mixed layer illite/smectite; K=kaolinite; Q=quartz; R=rectorite.

[4]The mineralogy of the clay-size fraction (<2μm) is very constant between samples, with the exception of the presence of calcite. The clay-size fraction is composed primarily of the following clay minerals: mixed-layer illite/smectite, discrete illite, and kaolinite. The illite/smectite has an expandability that lies between 80-90 percent. There may or may not be a very small amount of chlorite present in some samples. Other minerals in the clay-size fraction include calcite in some samples, quartz, and a small amount of feldspar. The position of the illite/smectite 001 of the air-dried sample is sensitive to interlayer chemistry: a 001 close to 12.5 Å would indicate Na^+ as the dominant exchange ion, whereas a spacing close to 14 Å would indicate a divalent ion such as Ca^{2+}. Most of the 001 positions indicate that the exchange cations predominantly are divalent. This interlayer chemistry would tend to limit the swelling potential of these clays.

[5]The metallic minerals observed in seams parallel to shale bedding, typified by sample 8, were determined by an SEM semi-quantitative analysis. The analysis shows a fair amount of Mn and Fe in the sample.

TABLE 5. Physical properties data determined from trench and core samples – Colorado

Sample Depth (m)	ΔW[1] Pore Water Increase Percent	ΔP[2] Volume Increase Percent	Bulk Density g/cc	Moisture Content Percent	Porosity Percent	Saturation Percent	Grain Density g/cc	Atterberg Limits Liquid Limit	Atterberg Limits Plastic Limit
2.56	12.24	19.22	1.94	18.77	42.26	86.1	---	---	---
2.91	12.54	19.66	1.94	18.92	42.47	86.0	2.72	---	---
2.91	---	---	---	---	---	---	2.75	---	---
4.00	3.24	7.11	2.08	15.48	35.73	89.9	2.70	49	22
6.63	0.0	5.91	2.08	14.10	34.53	85.0	---	---	---
7.93	5.78	8.60	2.07	16.43	36.61	92.9	2.73	---	---
10.21	10.08	13.41	2.02	18.92	39.30	92.5	---	---	---
13.11	13.11	6.87	2.09	16.84	36.31	96.9	2.74	---	---
16.07	6.20	6.20	2.12	16.56	35.18	100.0	2.73	---	---
18.60	6.69	7.46	2.10	16.75	35.94	98.0	---	---	---
19.74	8.70	9.51	2.08	17.53	37.14	98.0	2.73	---	---
20.49	6.71	8.29	2.08	16.81	36.43	96.0	---	---	---
21.59	6.81	8.60	2.10	17.23	36.61	98.0	---	---	---
22.41	6.42	6.35	2.12	16.67	35.27	100.0	2.75	---	---
24.01	2.67	2.67	2.16	15.24	32.95	100.0	---	---	---
25.61	0.0	0.0	2.19	14.23	31.16	100.0	2.72	41	19
25.61	---	---	---	---	---	---	2.72	---	---

[1]ΔW = Pore-water volume increase compared to unweathered sample at 25.61 m.

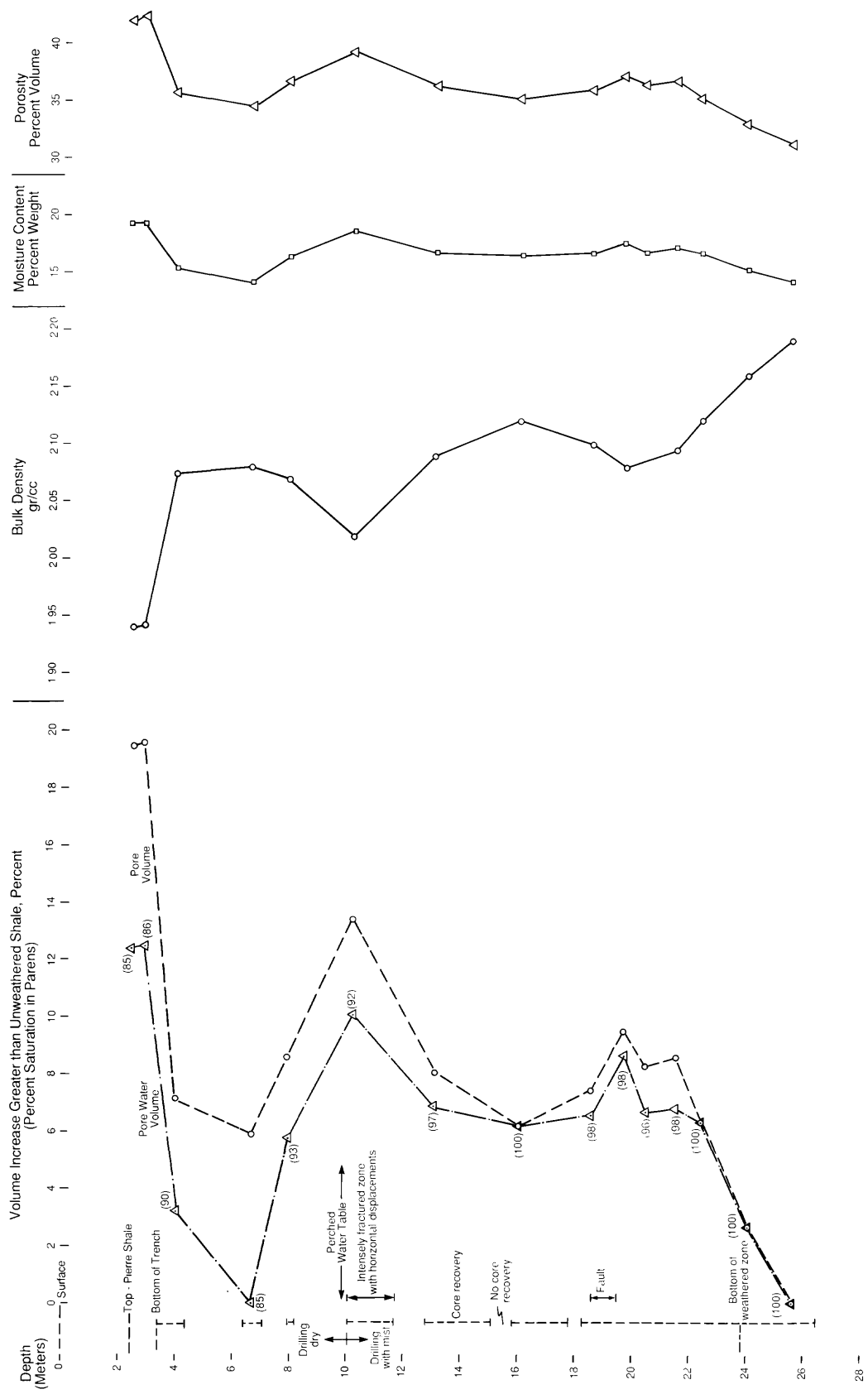[2]ΔP = Pore-volume increase compared to unweathered sample at 25.61 m.

Figure 5—Physical Properties, Pore Volume, and Pore Water Volume Change of the Pierre Shale vs. Depth

17

Because of apparent westerly thickening of the surficial deposits, the trench excavation began approximately 20 m east of the approximate location of the Golden fault trace, as mapped by Scott (1972), and 56 m north of Quincy Avenue. The core hole was located directly over the trench, 21 m northeast of the west end of the trench excavation, and was drilled to a depth of 27 m, 3 m below the deepest chemical weathering observed in the shale cores at 24 m. Air was used as a drilling fluid to a depth of 10 m where a perched water table was intercepted; below this, a heavy mist was used to the final depth of 27 m in order to obtain minimally disturbed core samples.

Three geologic units were mapped in the trench and are shown on the cross section in fig. 6 and described below. Additional descriptive information for unit 3 (Pierre Shale), taken from the drill-hole core logs, is also included. The cores, except for the vertical direction, are unoriented; therefore, strike directions of geologic structures observed in the cores are unknown.

Unit 1 is a modern, dark, humic-soil horizon, approximately 30 cm thick, developed on the present-day surface of Slocum Alluvium mapped by Scott (1972).

Unit 2 is a poorly sorted, pink to reddish-brown alluvial deposit containing numerous angular to well-rounded boulders (up to 1 m diameter), cobbles, and pebbles interspersed randomly in a fine-grained matrix consisting of micaceous, silty, fine- to medium-grained sand, having little or no stratification. The deposit, approximately 3 m thick and overlying the Cretaceous Pierre Shale, is mapped as the Slocum Alluvium (Scott, 1972) of Pleistocene age. At this location, the deposit was derived from the sedimentary and granitic rock of the adjacent uplifted Front Range of the Rocky Mountains and appears to have the composition and particle-size distribution similar to that of a complex debris flow (Varnes, 1978). The deposit is a heterogeneous mass of angular to well-rounded rock fragments within a fine-grained transporting matrix, indicating very rapid deposition.

Unit 3, the Upper Cretaceous Pierre Shale, is an upturned section of highly weathered marine shale with distinct bedding that strikes approximately N. 30° W. and dips between 65° and 90° northeast. Clay and bulk mineralogy, determined by Eberl (table 4), and grain-size distributions (Nichols, 1991) of the shale were determined from selected trench and core samples. With the exception of eleven distinct but irregularly spaced clayey to sandy seams parallel to bedding, the shale has a uniform lithology that consists of a yellow-brown to olive-gray smectitic clay (table 4) with finely interbedded silt and fine sand. As a result of weathering, the shale in the trench is oxidized and extensively fractured along bedding planes having occasional horizontal fractures; however, there is no visible evidence of a soil horizon developed in the shale below the sharp contact with the overlying Slocum Alluvium.

18

Figure 6–Geologic Cross Section of Trench Trending N68°E

19

The distinct seams mapped in the trench parallel to bedding (fig. 6) are contemporary to the shale deposition but have been modified by later erosion and weathering. All of these contain abundant fine-grained quartz and probably were deposited originally as fine-grained clayey, silty sand beds interlayered between the clay deposits within the Pierre Shale. After the shale was uplifted and tilted by Cenozoic tectonic activity, it is hypothesized that a period of subaerial weathering and erosion took place allowing an oxidized zone to develop in the tilted shale deposits. During the Pleistocene, probably during an interglacial sequence, M. Tuttle and D.S. Collins (oral commun., 1990) suggest that a reducing bog environment developed above the weathered surface of the tilted shale that allowed iron, manganese, and carbonate-rich, acidic-surface waters to percolate down through the fine-grained sand beds. Upon encountering the oxidized environment of the weathered shale, MnO, FeO, and $CaCO_3$ were precipitated in these beds. In addition, the percolating waters deposited and concentrated clay minerals derived from overlying shale deposits. The Slocum Alluvium was then deposited in such a forceful manner that it obliterated all vestiges of the existing surface environment on the shale. The mineralogy of the individual seams mapped in the trench, as analyzed by Eberl, is described in Nichols (1991).

Logs from the core hole show that the weathering profile of the shale extends gradationally to a depth of 24 m below the surface. The most severe weathering occurs to a depth of 10 m, where the drill intercepted a perched water table contained in a large fracture zone. Core recovered in this interval (27 percent) has nearly the same lithology (table 4) and appears to be nearly identical to the shale described in the trench except that there are fewer bedding-plane fractures and more horizontal fractures (vertical spacings of approximately 3 cm). These likely account for the poor core recovery.

Below 10 m depth, the shale lithology and clay mineralogy (table 4) is much the same, but the weathering gradually decreases with depth and core recovery increases from 58 percent at 13 m to 100 percent at 20 m. Cores from the 10-24 m interval are less oxidized and less fractured. Bedding-plane fractures are less numerous, but widely spaced (greater than 8 cm) horizontal fractures and high-angle conjugate shear fractures are dominant. Typically, many of the high-angle shear fractures and some of the horizontal fractures below 18 m are filled with gypsum 2-4 mm thick. Two zones of highly fractured and deformed rock are in the weathered profile at 10-11.5 m and at 18.3-20.0 m.

The shallower zone, between 10 m and 11.5 m, consists of brecciated shale interspersed between a series of nearly horizontal or low-angle fractures with an average spacing of approximately 4 cm (fig. 7). The breccia contains gouge and rotated rock fragments as large as 5 cm across. Although fault displacements could not be measured, some horizontal deformation was noted, and bedding-plane dip orientations were rotated at least 35° (from 80° to 65° in the opposite direction), indicating possible faulting in this zone.

Depth in Meters

11.59   11.28   10.97   10.67   10.36

← Vertical Up

BZ - Zones of brecciated shale showing fragmented shale

G-, Gouge Zones

Bedding planes of alternating shale and fine silty sand, and cross-cutting fractures

fractures

Figure 7–Drawing of Deformed Zones in Shale Cores from 10 to 12 meters depth

21

The deeper zone, between 18.3 m and 20.0 m, contains horizontal fractures, steeply dipping conjugate shear fractures, and has a fault dipping about 75° that cuts across the bedding. Because of the uniform lithology, displacements are nearly impossible to determine. The fault contains as much as 1.5 cm of compacted gouge that consists of ductilely deformed shale and rock fragments lightly bonded with a calcareous cement. In some locations, displacements have deformed the gypsum deposits filling previously formed fractures. The bedding above the fault dips approximately 65° in the opposite direction of the fault, and below the fault it is nearly vertical.

At 24 m depth, the boundary between the weathered and nonweathered shale consists of horizontal fractures with small drag folds, indicating some horizontal movement. Below 24 m to the end of the core hole at 27 m, the shale shows no signs of oxidation or chemical weathering. The only fractures observed were high-angle conjugate shear fractures and horizontal extensional fractures. The shear fractures cut across bedding planes and are covered with slickensides. None of the fractures contain gypsum filling.

Additional near-surface geologic information was obtained from the seismic-refraction profile (fig. 8). Under the drill-hole location, nearly horizontal refraction breaks are interpreted by Williams and King (in Nichols, 1991) to represent a soil layer to approximately 1 m depth, alluvium to approximately 2-4 m depth, drier shale to approximately 8 m depth, and saturated shale below 8 m depth. There is a vertical offset of about 2 m on the drier shale surface beyond the southwest end of the excavated trench.

Evidence for rebound

The field investigations in South Dakota and Colorado both show good evidence for rebound in the Pierre Shale, resulting from natural and engineering excavations. Even though the geologic setting and terrane of the shale at each location are somewhat different, the physical evidence for rebound is quite similar.

In addition to the vertical displacements observed along fault planes at the Oahe Dam stilling-basin excavations and along highways near Hayes, South Dakota, Nichols and others (1986) presented geotechnical evidence demonstrating the existence of relaxation between extensive lateral-rebound fracture zones (70 and 92 m deep) in the Pierre Shale of South Dakota. An analysis by Nichols and others (1986) and additional high-resolution seismic refraction data (Nichols and others, 1988) strongly suggest that the fracture zones were caused by rebound that resulted from the erosional unloading of overburden rocks.

Some of the geotechnical data show rebound responses of the shale caused by in situ loading and unloading. In core hole H13 (fig. 1), the inelastic
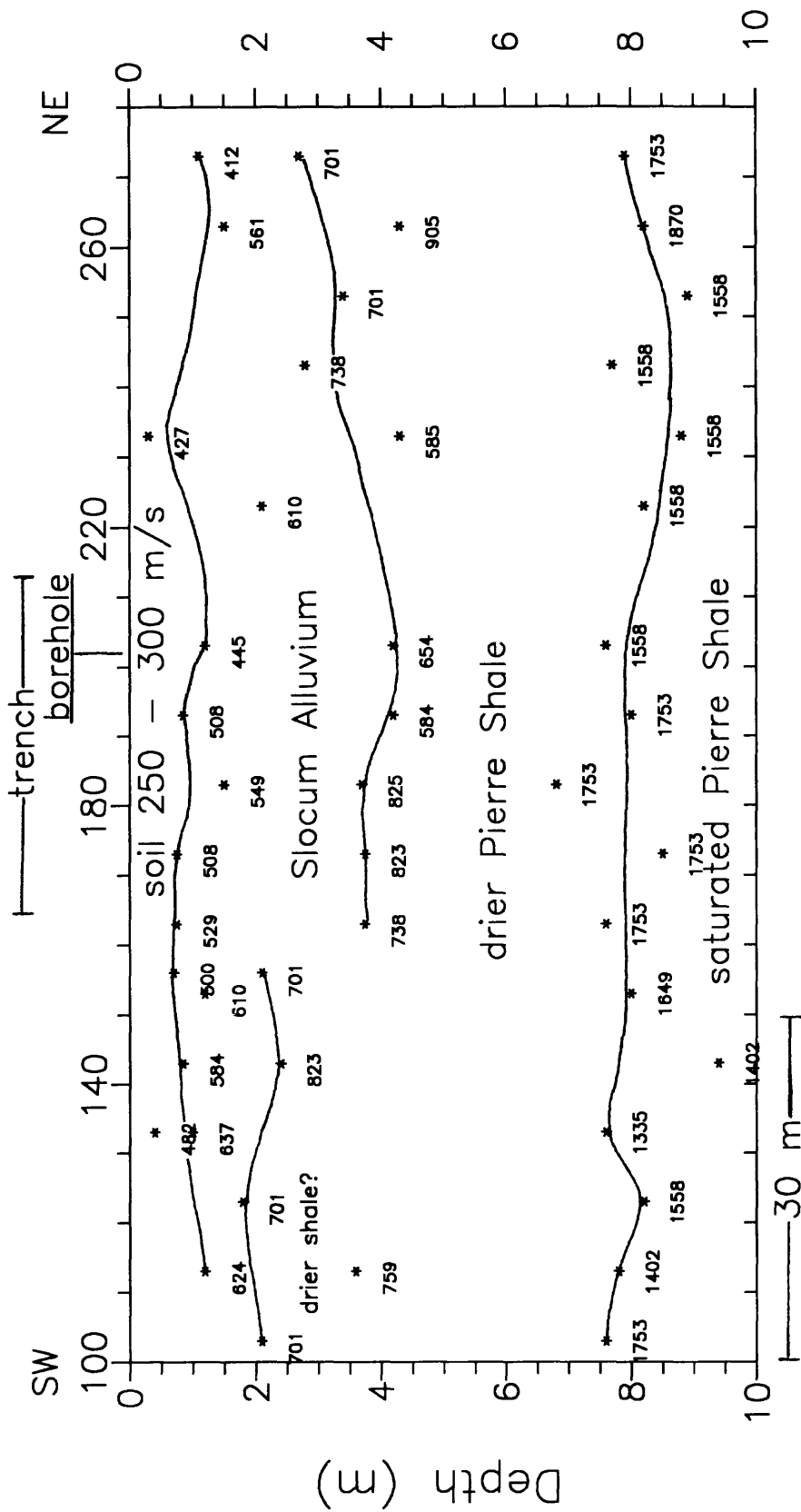
Figure 8–Depth section interpretation determined from the seismic refraction line (Fig. 4), identifying the four seismic layers and the calculated velocities (in meters per second) for those layers (Williams and King, 1991). The velocity annotated below each depth control point is applied over the interval from the control point above to the top of the next lower control point. 58:1 horizontal-to-vertical exaggeration.
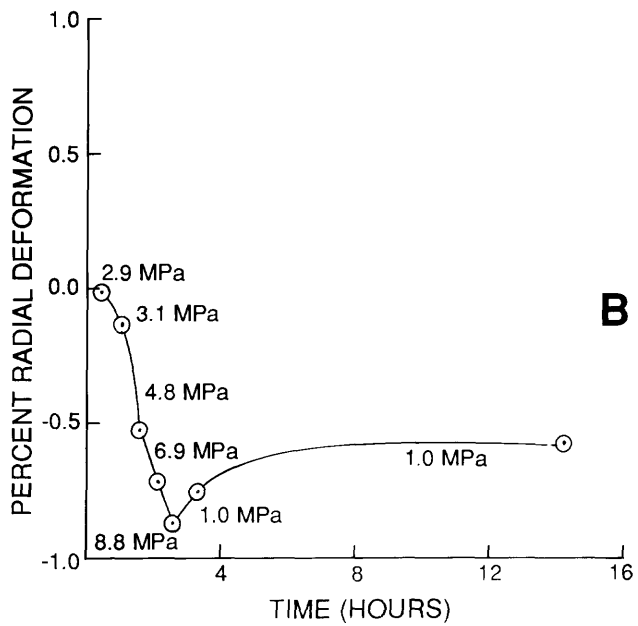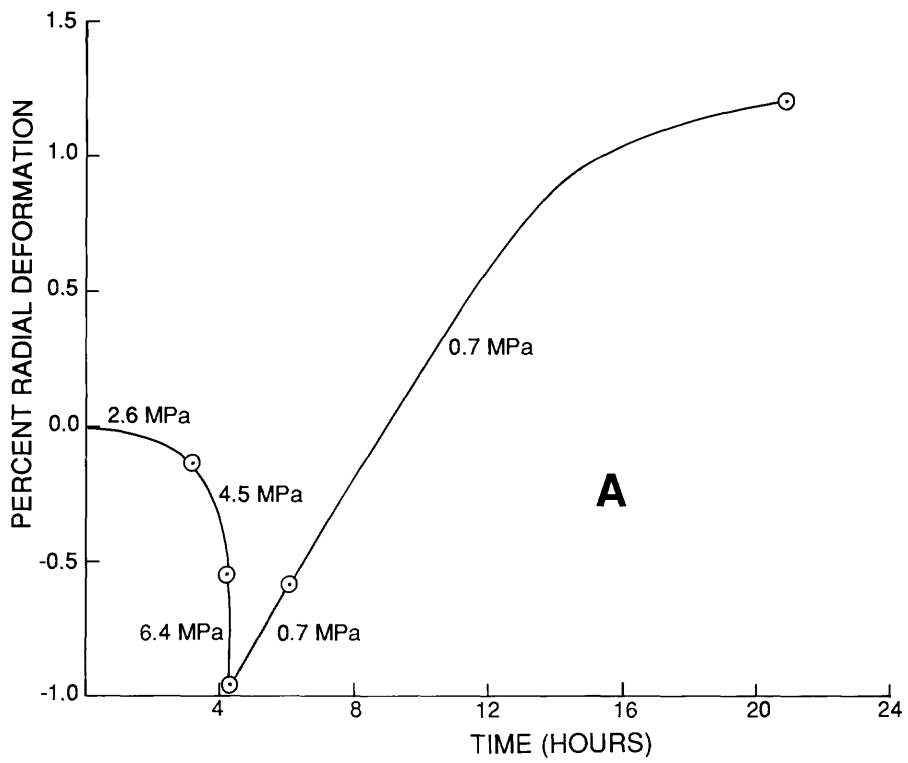
23

Figure 9–Creep curves determined <u>in situ</u> with pressuremeter tests. Numbers show increments of pressure applied to borehole wall by pressuremeter: (A) tested at 77 m, (B) tests at 108 m, in hole H13 (Fig. 1). (Adapted from Nichols and others, 1986).

time-dependent strain responses of bedrock, at depths of 77 and 108 m (fig. 9), were monitored when the core hole walls were incrementally pressurized with a pressuremeter to nearly five times the average horizontal in situ stress and then allowed to relax 16 to 24 hr at approximately one-half the average horizontal in situ stress. The initial pressurization at failure (fig. 9) broke down clay-particle bonds within the matrix, and the final reduction of pressurization allowed relaxation of the matrix. The larger relaxation response seen on the 77-m test, located between two naturally occurring rebound fracture zones at 70 and 92 m depth, was attributed to previous partial matrix relaxation caused by the natural rebound-induced fractures, whereas the test at 108 m was well below the fracture zones, in shale with an unrelieved matrix. In addition, vertical strain relaxation of as much as 1.5 percent in the shale caused by the removal of cores from 15 to 33 m of overburden loads in core holes H8, 10, 11, and 12, is demonstrated by the total time-dependent strain response of these cores for 42-48 hr after coring (fig. 10). The larger strains measured on cores from 15-23 m depth infer greater relaxation of fabric at these depths. These data illustrate the time-dependent expansive nature of inelastic rebound caused only by the loading and unloading of the rock mass. It follows that measurable physical changes must relate to these short-term rebound displacements, the most notable being volume change. Because the above experiments are of such short-term nature, it is doubtful that significant pore-water transfer or chemical changes occur, as they do in the long-term rebound and deterioration of rocks. Rebound displacements result from expansion that occurs upon the breakdown of the clay-particle matrix compressed and lithified during sedimentation and diagenetic processes. The expansion has been explained by Bjerrum (1967), who states the following regarding overconsolidated plastic clays: "The recoverable part of the compression is believed to be primarily the result of deformation of the flexible flake-shaped clay particles. When the load is removed, the particles tend to regain essentially their original shape, provided they were not strained beyond their elastic limit. When a clay has been consolidated under a given pressure, it contains a certain amount of what may be called recoverable strain energy." According to Bjerrum, strain energy is locked in the shale by diagenetic clay bonds, which, upon disintegration, allow the relief of the energy, causing expansion of the fabric.

The South Dakota data in tables 1 and 2 and in fig. 3 show that the unweathered shale samples from the core hole are always totally saturated, more dense, less porous, and containing less water than the weathered samples from the shallow trenches. The weathered samples always have higher water content but are not saturated, whereas the unweathered samples are saturated. The data therefore imply that the shallow weathered samples have increased in volume and water content, but that the moisture inflow does not completely fill new void space. The volume expansion is attributed to the release of recoverable strain energy that results when overburden is excavated by erosional processes (Nichols and others, 1986) and in part possibly to expansion caused by hydration of the clay.
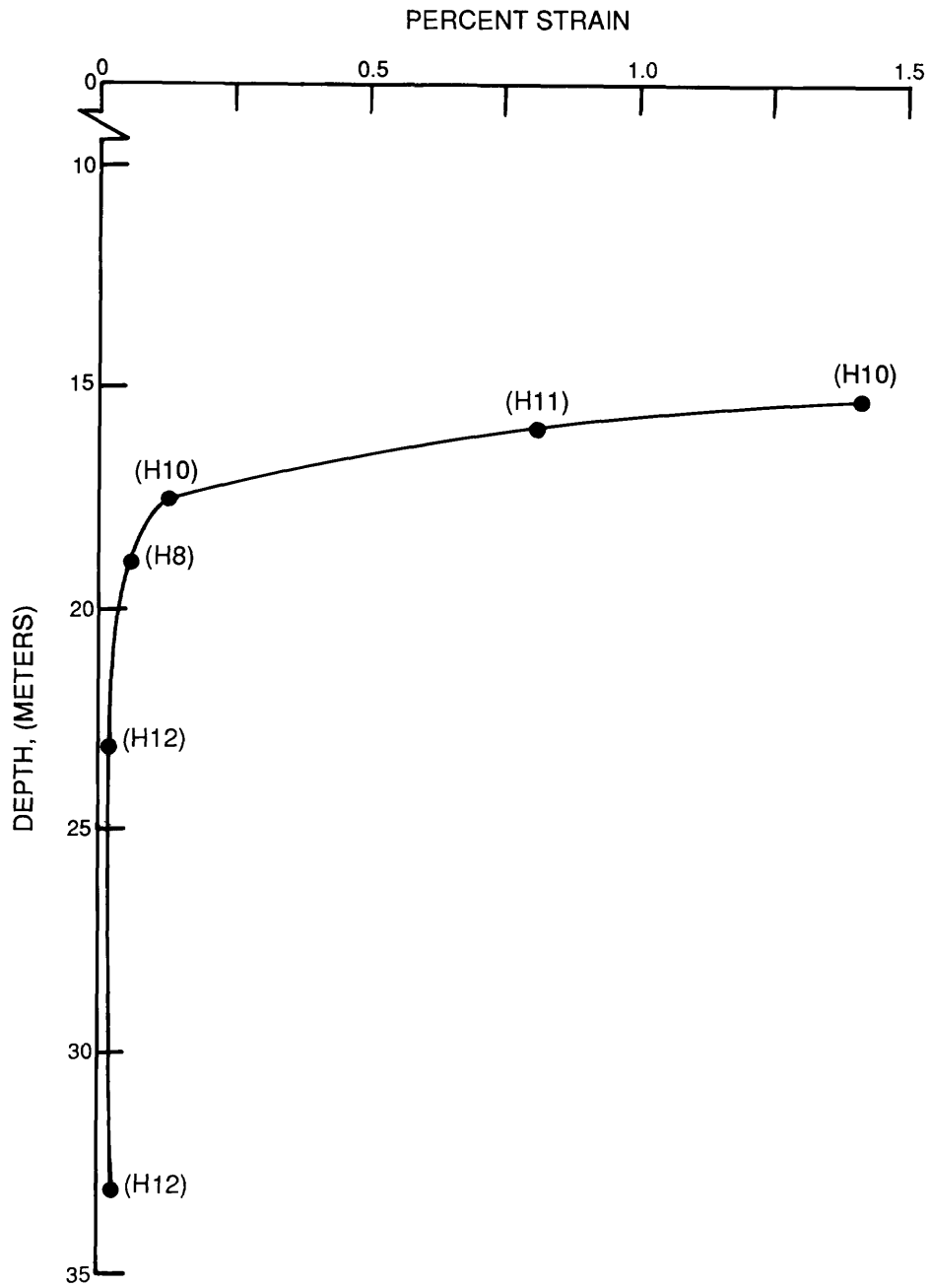
Figure 10–Maximum cumulative vertical rebound strain for 48 hours on selected cores versus depth. Hole numbers (see Fig. 1) are shown next to data points. (Adapted from Nichols and others, 1986).

A natural profile in the shale that has resulted from erosional excavation of overburden was developed at the Colorado site. Since the top surface of the Pierre Shale was visually devoid of a recognizable soil horizon, swelling soil properties could not be evaluated, but the data obtained allow an evaluation of past natural rebound and potential rebound damage to structures caused by construction practices.

Since excavations are directly above the rebounded shale that is still horizontally confined, most expansion takes place vertically, and the resulting increase of volume is increased void space that absorbs available ground water through a disintegrating but more permeable matrix. The unweathered shale below 24 m depth experienced very little alteration or rebound expansion and, therefore, the clay fabric is still relatively intact. As in South Dakota, the unweathered samples taken from this depth, when compared to shallower weathered samples, are the most dense and contain the least water, even though they are completely saturated (fig. 5).

The clay mineralogy of the unaltered shale has slight differences of exchangeable cations from those in the weathered shale sampled above. There is a perceptible decrease of smectite expandability (90 to 80 percent) in the weathered clays above 24 m depth (Nichols, 1991), an indication of the increase of the divalent ion Ca^{2+} obtained from permeating ground water in fractures and sandy layers. The dominance of the divalent cation in the smectite/illite 001 layer tends to stabilize the hydration layer at about 15Å until saturation is attained and then stabilizes at 19Å (MacEwen and Wilson, 1980), thereby inhibiting further hydration. The calcium-rich waters also enhanced the precipitation of gypsum in fractured zones of the weathered rock.

Although rebound deformations probably have occurred deeper, other physical property measurements from the Pierre Shale of Colorado (Collins and Nichols, 1987) and South Dakota (Nichols and others, 1986) indicate very little expansive volume change in the unaltered, saturated rock below the weathered zone except where there is extensive fracturing or faulting. Sample properties from the 26 m depth, therefore, are used to represent the relatively undisturbed conditions of the shale prior to destructive rebound deformations. All of the properties determined on the remaining core samples taken above this depth are used for a comparison of the volume changes that have occurred at shallower depths (fig. 5). (Sample volume-increase calculations are shown in Appendix C of Nichols, 1991).

Above the undisturbed shale at the 26 m depth, the volume shows increases of approximately 6.4 percent up to the 22 m depth, where it is locally affected by a fault zone (fig. 5) from 22 to 18 m. Above this depth, the volume remains approximately constant (6-8 percent greater than undisturbed samples) up to a depth of 4 m, except in the fracture zone containing the perched water table at 10 m. Above 4 m, there is nearly a 20-percent volume increase at less than 2 m below the shale-alluvium contact.

Between 18 m and 22 m, there is an 8-10 percent volume increase associated with a fault zone. Between 7 m and 12 m, there is an 8-14 percent volume increase associated with a horizontally displaced fracture zone containing a perched water table.

The pore-water content increases with decreasing depth in a similar manner to the pore-volume increase, except that it is progressively less than the pore-volume increase; thus, the saturation of the cores becomes progressively less toward the surface (fig. 5). Also, the pore-water content and pore volume have similar increases related to the fracture, fault zones, and perched water table. Based on the described patterns of pore and pore-water-volume increases, the volume of the slightly weathered shale above the undisturbed shale initially rebounds, maintaining saturation up to a depth of 22.4 m. Sufficient pore water is still available here to completely fill the increased pore space. The 6.4 percent rebound at this depth results from the release of recoverable strain energy caused by weathering-induced relaxation of diagenetic clay and chemical bonds (Bjerrum, 1967; Russell and Parker, 1979) and possible additional swelling as available ground water is absorbed by clays. However, the illite/smectite clays at this depth, showing a slight increase of the Ca^{2+} cation, probably have stable hydrated intercrystalline layers of the 001 spacing at 14-15 Å (Nichols, 1991, Appendix A). Typically, these clays remain stable at 15 Å from 20 to about 85 percent relative humidity until they become saturated and then are stable at a 19 Å spacing (MacEwan and Wilson, 1980), thereby limiting any further hydration. Above 22 m depth, however, expansion exceeds the ability of available pore water to flow in, leaving the shale only partially saturated. Because the initially saturated 14-15 Å clays are likely to remain stable and the hydrated layers may collapse as they become less saturated, thus, they probably do not contribute significantly to the expansion. Also, as the shale above 22 m becomes progressively less saturated, it is doubtful that osmotic pressure gradients contribute to the rebound volume expansion.

A very distinct increase of rebound and increased pore-water volumes in the vicinity of the fault, perched water-fracture zones, and the very shallow, highly weathered shale (fig. 5) indicate that these features greatly enhance the rebound process. Between 18 m and 21 m, the faulted shale along gypsum and gouge-filled fractures appears to have had displacements both before and after the gypsum emplacement. Disruption and dilation of the shale fabric during repeated faulting has allowed relaxation of diagenetic clay (Nichols and others, 1986) and chemical bonds in addition to that produced by weathering (Russell and Parker, 1979), thereby permitting recoverable strain energy to cause subsequent volume increases. However, the lateral confining pressure at the 18-21 m depth does not permit a very large rebound volume (only about 8-10 percent greater than the undisturbed shale); even so, there is either an insufficient source of pore water or the permeability of the shale is so low that the vacant pores become only partly filled, thereby leaving the shale only partially saturated (96-98 percent). Between 7.5 m and

12.7 m (the highly fractured zone containing a perched water table), volume rebound exceeded 13 percent of the undisturbed shale and, again, the available pore water was unable to fill the vacant pores (fig. 5). The decreased confining pressure at this shallower depth allowed substantially larger rebound volume, but the saturation was only 92.5 percent, even though a perched water table was present. Above the 7.5 m depth, the shale in the upper part of the weathered zone is highly fractured with minimum confinement, and the volume rebound near the upper shale boundary approaches a 20 percent increase over that of the undisturbed shale (fig. 5). This is the largest expansion for the total profile, yet it has the lowest saturation (only 86 percent) and, again, the available moisture is unable to fill the increased pore volume.

The rebound represented by increasing pore volume on this profile becomes greater towards the surface, as the confining pressure decreases. Locally, geotechnical measurements indicate that rebound appears directly related to the degree of disintegration in the clay matrix caused by weathering and fracturing; that is, maximum expansion occurs in the highly fractured and weathered zones nearest to the surface. The in-situ physical properties measurements and experiments performed by mechanical pressurization of core hole walls in the Pierre Shale of South Dakota (fig. 9) demonstrated the occurrence of time-dependent expansion of bedrock caused by fracturing and unloading the in-situ shale (Nichols and others, 1986; Nichols, 1991).

The pore-water content also increases toward the surface and in the highly deformed zones, but is decreasingly able to maintain saturation of the increased pore volume and, therefore, may not cause further swelling of the already stable hydration state of the 14-15 Å clays. Even in zones of fabric deterioration caused by fracturing and faulting where pore water may be abundant, saturation of the clay matrix is not maintained, which suggests that absorption does not keep up with the rate of volume increase. Therefore, the volume increase logically precedes the inflow of pore water that may be accommodated by increased permeability. Notice that at the 6.6 m depth above the perched water table, there has been a 6 percent volume increase but no increase of pore water to fill the vacant voids (saturation only 86 percent), indicating that at this location, the shale above the perched water table is not accessed by fracture aquifers supplied by surface runoff. This implies that the fracture zone and perched water table existing below are associated with a vertical fracture system at some other location than at our drill-hole profile. In addition, the volume expansion profile (fig. 5) appears to be independent of the clay mineralogy, which remains relatively constant for the suite of samples tested from the vertical profile.

Based on the seismic-refraction data (fig. 8), the horizon at 4.2 m depth just below the Slocum Alluvium-Pierre Shale contact contains a distinct offset (approx. 2 m) between stations 155 and 160. The offset, however, does not appear to exist on the deeper refraction horizon at 7.5 m just above the

fracture zone and perched water table, but there is an anomalous refraction point here. Movement on the Golden fault, approximately located off the SW end of our trench (fig. 4), may have caused displacement of the shale-alluvium contact. If this is the case, then the horizontal fracture zone and perched water table appear to postdate or develop penecontemporaneously to singular or recurrent fault movements. The anomalous refraction on the lower horizon may represent movement on a local structure created by recurrent fault movement. The zone is nearly horizontal for the length of the refraction profile, and the drill cores demonstrate evidence of horizontal deformation (fig. 7), thus indicating the possibility that faulting or erosional rebound associated with faulting may have been responsible for the fracture zone (Nichols and others, 1986). The perched water table along the horizontal fracture zone may be fed by meteoric water infiltrating along a vertical fracture zone, possibly associated with faulting.

The data on the profile demonstrates the probability that any removal of overburden down to 4 m is likely to be followed by expanding bedrock with a volume increase as much as 14 percent of the unweathered clay, mostly in a time-dependent or ductile manner. This kind of time-dependent behavior has been demonstrated on newly extracted cores removed from shallow depths (fig. 10) in the Pierre Shale of South Dakota (Nichols and others, 1986), also by time-dependent rebound after excavation of the shale for highway construction (Collins and others, 1988) and by rebound on the stilling-basin floor during construction of the Oahe Dam in South Dakota (Underwood and others, 1964).

Conclusions

The data gathered from this investigation deal mostly with the understanding of natural rebound in the Pierre Shale that has resulted from the erosional removal of overburden. The profile of physical properties, and mineralogical and geological descriptions that help to define influences of geologic structures and the progression of natural rebound in a vertical section, permit a prediction of problems that may occur with the removal of overburden by engineering excavations and disturbances. Upon removal of any of the upper weathered shale or covering alluvial deposits, time-dependent rebound probably will occur within the shale. The amount of rebound at the surface depends on the amount of overburden excavated; the amount of rebound that already has occurred in the shale below the excavation; the degree of saturation; the existence of faults, fracture zones, or any other geologic structures causing major bedrock inhomogeneities; the condition of rebound equilibrium prior to excavation; and the depth and content of alluvium still remaining above the shale. In addition, the amount of rebound will depend on the constraint of the engineered structures built on the excavation site and the type and amount of fill added above the excavation surface.

30

The effects of engineering construction on the rates and displacements produced by rebound at the excavation surface are impossible to predict without post-excavation displacement measurements. Additional geotechnical measurements are needed to evaluate the effects of degree of saturation, existence of bedrock fracturing and faulting, remaining bedrock rebound potential, and restraints caused by structural loading.

References

Bjerrum, L., 1967, Progressive failure in slopes of overconsolidated plastic clay and clay shales: American Society of Civil Engineers Journal of the Soil Mechanics and Foundations Division, 93(SM5), p. 3-49.

Collins, D.S., and Nichols, T.C., Jr., 1987, Preliminary data report conducted for the Colorado State Geological Survey on the Superconducting Supercollider Study: U.S. Geological Survey Open-File Report 87-55, p. 1-13.

Collins, D.S., Swolfs, H.S., and Nichols, T.C., Jr., 1988, Highway damage related to faults near Pierre, South Dakota: U.S. Geological Survey Open-File Report 88-674, 42 p.

Crandell, D.R., 1958, Geology of the Pierre area, South Dakota: U.S. Geological Survey Professional Paper 307, 83 p.

Kirkham, R.M., and Rogers, W.P., 1981, Earthquake potential in Colorado: Colorado Geological Survey Bulletin 43, p. 1-171.

Kline, J.H., 1982, Natural and man-made factors that influence property damage due to swelling soils in southeastern Jefferson County, Colorado: Golden, Colorado School of Mines M.S. thesis, 182 p.

MacEwan, D.M.C., and Wilson, M.J., 1980, Interlayer and intercalation complexes of clay minerals, Chapter 3 in Brindley, G.W., and Brown, G., eds., Crystal structures of clay minerals and their X-ray identification: London, Mineralogical Society Monograph No. 5, p. 197-248.

Nichols, T.C., Jr., 1980, Rebound, its nature and effect on engineering works: Quarterly Journal of Engineering Geology, 13, p. 133-152.

_____1991, Investigation of foundation problems related to heaving of soils and weathered bedrock in the Pierre Shale southwest of Denver, Colorado: U.S. Geological Survey Open-File Report 91-281, 50 p.

Nichols, T.C., Jr., and Collins, D.S., 1986, In situ and laboratory geotechnical tests in the Pierre Shale near Hayes, South Dakota: U.S. Geological Survey Open-File Report 86-152, 24 p.

_____1991, Rebound, relaxation, and uplift, in The Heritage of Engineering Geology--The First Hundred Years, 1888-1988: Geological Society of America, Centennial Special Volume 3, Chapter 11, Part II, p. 265-276.

Nichols, T.C., Jr., Collins, D.S., and Davidson, R.R., 1986, In-situ laboratory geotechnical tests of the Pierre Shale near Hayes, South Dakota--A characterization of engineering behavior: Canadian Geotechnical Journal, 23, p. 181-194.

Nichols, T.C., Jr., King, K.W., Collins, D.S., and Williams, R.A., 1988, Seismic-reflection technique used to verify shallow rebound fracture zones in the Pierre Shale of South Dakota: Canadian Geotechnical Journal, 25, p. 369-374.

Russell, D.J., and Parker, A., 1979, Geotechnical, mineralogical, and chemical interrelationships in weathering profiles of an overconsolidated clay: Quarterly Journal of Engineering Geology, 12, p. 107-116.

Scott, G.R., 1972, Geological map of the Morrison Quadrangle, Jefferson County, Colorado: U.S. Geological Survey Miscellaneous Investigations Map I-790-A, scale 1:24,000.

Underwood, L.B., Thorfinnson, S.T., and Black, W.T., 1964, Rebound in design of Oahe Dam hydraulic structures: American Society of Civil Engineers Journal of the Soil Mechanics and Foundations Division, 90(SMI), p. 1-27.

Varnes, D.J., 1978. Slope movement types and processes, in Schuster, R.L., and Krizek, R.J., eds., Landslides, analysis and control: Transportation Research Board, National Academy of Sciences, Special Report 176, 234 p.

Williams, R.A., and King, K.W., 1991, A seismic investigation of shallow surface layers near Friendly Hills Subdivision, Denver, Colorado, Appendix B in Nichols, T.C., Jr., Investigation of foundation problems related to heaving of soils and weathered bedrock in the Pierre Shale southwest of Denver, Colorado: U.S. Geological Survey Open-File Report 91-281, p. 25-33.